Journal of
Mechanical
Science and
Technology

Journal of Mechanical Science and Technology 21 (2007) 505~512

A Study on Heat Transfer Characteristics for Staggered Tube Banks in Cross-flow

Seong-Yeon Yoo[a], Hwa-Kil Kwon[b,*], Jin-Hyuk Kim[a]

[a]*BK21 Mechatronics Group, Chungnam National University, Daejeon 305-764, Korea*
[b]*Mechanical Engineering Research Institute, Korea Advanced Institute of Science and Technology, Daejeon 305-701, Korea*
BK21 Mechatronics Group, Chungnam National University, Daejeon 305-764, Korea

(Manuscript Received August 2, 2006; Revised December 9, 2006; Accepted January 10, 2007)

Abstract

Cross-flow over tube banks is commonly encountered in practice in heat transfer equipments. The local and average heat transfer characteristics for staggered tube banks are investigated in the present study. A naphthalene sublimation technique is employed to obtain the local heat transfer coefficients, and experiments are performed for various tube spacings, tube locations and Reynolds numbers. The variation of the local heat transfer coefficients is quite different from the first tube to the third tube, but they are similar afterwards. The average Nusselt number increases more than 30% and 65% on the second and third tubes, respectively, in comparison with that of the first tube. And the empirical correlations for average heat transfer coefficients are compared with the conventional heat transfer correlations.

Keywords: Heat transfer characteristics, Staggered tube banks, Naphthalene sublimation technique, Heat and mass transfer

1. Introduction

Cross-flow over tube banks is commonly encountered in practice in heat transfer equipments such as the condensers and evaporators of power plants, refrigerators, and air conditioners. In such equipment, one fluid moves through the tubes while the other moves over the tubes in a perpendicular direction. Numerous experimental and numerical investigations have been conducted on the flow and heat transfer for a single tube or tube banks. In case of the experimental studies, many previous works mainly concerned with overall heat transfer through the banks (Pierson, 1937 ; Huge, 1937 ; Grimison, 1937). Žukauskas (1972) reviewed flow and heat transfer characteristics for a single cylinder and tube banks. Achenbach (1989) measured the integral and local heat transfer from only one staggered tube bank at high Reynolds numbers ($\mathrm{Re} \geq 10^5$), and investigated the locations of boundary layer separation and transition to turbulence. Aiba et al. (1982a, 1982b) measured the heat transfer coefficients, velocity profile and turbulence intensity around tubes for in-line and staggered arrangements of tube banks in the Reynolds number of 10^4 to 6×10^4, and discussed the heat transfer characteristics in connection with the fluid flow behavior. Kim et al. (2000) experimentally studied the effect of scale roughness, cylinder spacing and Reynolds number on the heat transfer around only the third cylinder in the staggered tube banks. Merker and Hanke (1986) performed mass transfer experiments using the naphthalene sublimation technique for the shell side of tube banks having oval-shaped tubes, but obtained only average Sherwood numbers. Most of the numerical studies have been carried out at relatively low Reynolds numbers as it is difficult to predict exact flow and heat transfer around cylinders due to complex flow phenomena. Park et al.

*Corresponding author. Tel.: +82 42 869 3066, Fax.: +82 42 869 8207
E-mail address: s_garcon@kaist.ac.kr

(1998) simulated the flow past a circular cylinder at Reynolds numbers up to 160, and compared their results with the previous experimental and numerical results. Buyruk et al. (1998) numerically studied flow and heat transfer on a single cylinder as a function of blockage ratio for Reynolds numbers of 120 and 390. Buyruk (2002) predicted the heat transfer characteristics in tube banks with tube arrangement and flow condition at low Reynolds numbers below 4×10^2.

When fluids pass through tube banks, complex flow phenomena such as stagnation, separation, reattachment, vortex formation or recirculation affect the local heat transfer characteristics. In complicated flow situations, it is very difficult to measure local heat transfer coefficients by conventional heat transfer measurements. In the present study, a naphthalene sublimation technique is employed to measure the local mass transfer coefficients, and they are converted to their counterpart of heat transfer process using the heat/mass transfer analogy. In heat transfer experiments, measured data generally include conduction and radiation losses. But with the naphthalene sublimation technique, these errors can be eliminated and more detailed data can be obtained.

The purpose of this study is to investigate the local and average heat transfer characteristics at various tube spacings, tube locations and Reynolds numbers for staggered tube banks in cross-flow. The empirical correlations for average heat transfer are obtained by integrating the local heat transfer coefficients and they are compared with the conventional heat transfer correlations.

2. Experimental apparatus and procedure

2.1 Experimental apparatus

The experimental apparatus consists of a wind tunnel, naphthalene casting facility, automated sublimation depth measurement system and tube bank. A suction type wind tunnel is used, which has a rectangular cross section of 400 mm wide $\times$300 mm high. The maximum air speed in the wind tunnel is 25 m/s, and the free-stream turbulence intensity is less than 0.5% over the entire range of speed.

The automated sublimation depth measurement system comprises a depth gage along with a signal conditioner, two stepping motor-driven θ-z traversing table, a hardware unit for motor control and a data acquisition system. The depth gage used to measure the naphthalene surface profile is a linear variable differential transformer (hereafter LVDT) which has $\pm$0.254 mm linear range and 25.4 nm resolution. It is connected to a signal conditioner which supplies excitation voltage to the LVDT and amplifies the output signal from the LVDT. For precise and automatic positioning of the LVDT on the test tube, the LVDT and test tube are tightly mounted on the θ-z traverse table, and two stepper motors move them. The data acquisition system equipped with a personal computer controls the movements of step-ping motors and gets the data from the signal con-ditioner.

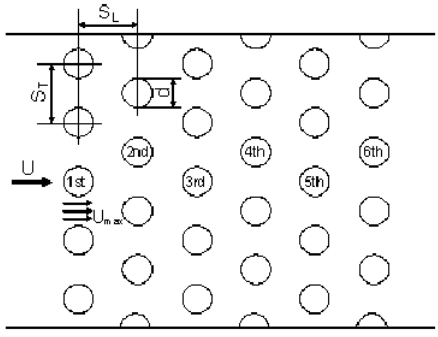

Fig. 1. Schematic of staggered tube banks.

The test tube cast with naphthalene, which is actually circular rod of stainless-steel, and has a size of 192 mm length $\times$ 30 mm diameter with 1.5 mm groove. The staggered tube bank, as shown in Fig. 1, has six rows and five tubes for each row. All the dummy tubes made of acrylic plastic are 30 mm in diameter. Three relative transverse and longitudinal tube spacings are examined; that is, $S_T/d(=S_L/d) = 2.0$, 1.75, 1.5. The location of the naphthalene-casted tube is varied from the first tube to the sixth tube to obtain the local heat transfer coefficients for each tube location.

2.2 Experimental procedure

A new naphthalene casting is made for each test run, and the properties of naphthalene are given in Table 1. The test tube is assembled into the mold, and molten naphthalene is then poured into the mold. After the naphthalene solidifies and cools down to room temperature, the mold is separated from the test tube by applying a shear force. The naphthalene-casted tube is placed and clamped on the measurement table. Initial readings of the naphthalene surface profile are taken at predetermined locations using the data acquisition system. The test tube is then installed

Table 1. Properties of naphthalene.

Molecular formula	$C_{10}H_8$
Molecular weight	128.17
Melting point	80.2℃
Density	1,162 kg/m^3
Thermal conductivity	0.333 W/mK

in the wind tunnel and exposed to the air stream for about one hour. During a test run, tunnel air temperature is measured using a RTD (Automatic Systems Laboratories, F250 Precision Thermometer), and free-stream velocity is measured using a pitot tube. The temperature on the naphthalene surface is almost same as the air temperature. After blowing, the test tube is removed from the wind tunnel, and a second set of surface profile is measured at the same locations as before. Finally, local and average Nusselt numbers are calculated from the measured naphthalene surface profile and other related data using the data reduction program. The experiments are performed for various tube spacings ($S_T/d=S_L/d$ = 2.0, 1.75, 1.5), tube locations (from the first tube to the sixth tube) and Reynolds numbers (from 7,700 to 30,300).

3. Data reduction

The mass transfer coefficient is defined by

$$\dot{m}/A = h_m(\rho_{v,w} - \rho_\infty) \tag{1}$$

where $\dot{m}$ is the mass transfer rate, A is the naphthalene sublimation area, h_m is the mass transfer coefficient, $\rho_{v,w}$ is the naphthalene vapor density on the surface, and ρ_∞ is the naphthalene vapor density in the free-stream, which is ignored in this study. The empirical equation of Ambrose et al. (1975) is used to determine the naphthalene vapor pressure and the naphthalene vapor density on the surface is then evaluated from the ideal gas law.

The local mass transfer rates are determined from

$$\dot{m}/A = \rho_s \Delta t / \Delta\tau \tag{2}$$

where ρ_s is the density of the solid naphthalene, Δt is the net sublimation depth, and $\Delta\tau$ is the total exposure time in the wind tunnel. Total naphthalene sublimation depth is calculated from the measured surface profiles before and after the exposure in the wind tunnel, and the excess sublimation due to natural convection during the surface profile measurement is subtracted to get the net sublimation.

Combining Eqs. (1) and (2) gives

$$h_m = \frac{\rho_s \Delta t / \Delta\tau}{\rho_{v,w}} \tag{3}$$

The mass transfer coefficients obtained from Eq. (3) can be expressed in terms of dimensionless form, Sherwood number as defined in Eq. (4).

$$Sh = h_m d / D_{iff} \tag{4}$$

where d is the cylinder diameter. The mass diffu-sion coefficient of naphthalene in the air, D_{iff} is determined from the correlation recommended by Goldstein and Cho (1995).

The measured mass transfer coefficients are converted to their counter part of heat transfer process using the following heat and mass transfer analogy relation,

$$Nu/Sh = (Pr/Sc)^n \tag{5}$$

where 1/3 is used for exponent n in this study. According to the uncertainty analysis suggested by Kline and McClintock (1953), the estimated error of Nusselt number is about 7.4%.

4. Results and discussion

4.1 Local heat transfer characteristics

In order to get the local heat transfer coefficients, the naphthalene surface profile is measured at the interval of 5° in the circumferential direction, and 11 data are obtained in the axial direction for the length of 10 mm of the tube.

Figure 2 shows the distribution of local Nusselt numbers for the single tube. As shown in Fig. 2(a), the distinct variation of the local heat transfer coefficients is observed in the circumferential direction, but they are nearly constant in the axial direction. Two dimensional plot of Fig. 2(b) is obtained by averaging the three dimensional Nusselt numbers in the axial direction. In this figure, the angle(θ) is measured from the front stagnation point, and 180° denotes rear stagnation point. The maximum heat trans-

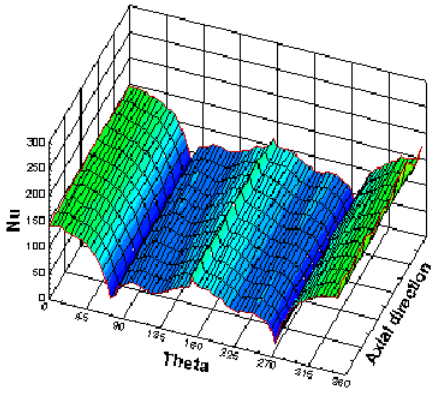

(a) 3-dimensional plot

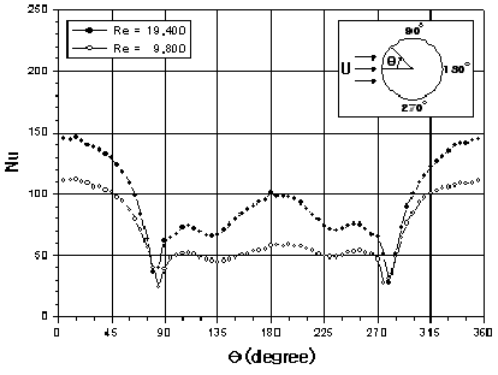

(b) 2-dimensional plot

Fig. 2. Distribution of local Nusselt number for single tube.

transfer coefficient appears at the front stagnation point, and then the heat transfer coefficients decrease gradually as the boundary layer grows. The separation point at which the heat transfer coefficient has minimum value is found near θ=85°. The small valley of the local heat transfer coefficients is observed near θ=135°, which may be due to the upwash secondary vortices (Son and Hanratty, 1969; Boulos and Pei, 1974). After that, the heat transfer coefficient goes up again due to the strong mixing of fluids and the vigorous motion of turbulent eddy. As Reynolds number which is based on the approaching velocity(U) increases, the local heat transfer coefficients increase. However, there is no significant change in their distribution pattern.

The local Nusselt numbers are investigated for tube spacings of $S_T/d=S_L/d=2.0$, 1.75, 1.5 when the approaching velocity is 4 m/s, and the location of the naphthalene-casted tube is changed from the first row to the sixth. Fig. 3 presents the distribution of the local Nusselt numbers at various tube locations for three tube spacings. In the figure, Reynolds number is defined as follows (Fig. 1).

$$Re = \frac{U_{\max} d}{\nu} \tag{6}$$

where $U_{\max}$ is the maximum velocity between tubes as defined by Eq. (7).

$$U_{\max} = \frac{S_T}{S_T - d} U \tag{7}$$

In case of $S_T/d=S_L/d=2.0$ shown in Fig. 3(a), the local heat transfer coefficients of the first tube are much lower than those of other tubes. They are entirely similar to those of the single tube but the separation point is shifted about 10° downstream due to the blockage effect of nearby tubes (Scholten and Murray, 1998). In the second tube, the local heat transfer coefficients increase considerably compared to those of the first tube because the approaching velocity becomes almost double compared to the first row. Two minimum heat transfer values appear at about θ=90° and 150°. The first heat transfer minimum corresponds to the transition to turbulence within the boundary layer, and the second minimum means the separation of the turbulent boundary layer (Scholten and Murray, 1998; Žukauskas, 1972). For the third tube, the distribution of the local heat transfer coefficients is similar to that of the second tube, but higher heat transfer coefficients are observed especially in the front part of the tube. After the third tube, the distribution of the local Nusselt numbers shows little variation. This can be explained by the fact that flow is developed, and the flow pattern rarely changes after the third tube.

The effect of tube location on the local Nusselt numbers for tube spacings of $S_T/d=S_L/d=1.75$ and 1.5 is presented in Figs. 3(b) and 3(c), respectively. The distribution pattern of the local heat transfer coefficients on each tube from the first row to the sixth row is much similar independent of the tube spacing. As the tube spacing decreases, the variation of the local heat transfer coefficients is more distinct, and they increase in the whole domain except the first tube. The reason is that the maximum velocity between tubes increases with decreasing tube spacing, although the approaching velocity is constant at 4 m/s for all tube spacings. For all tube spacings, the average Nusselt number increases more than 30% and 65% on the

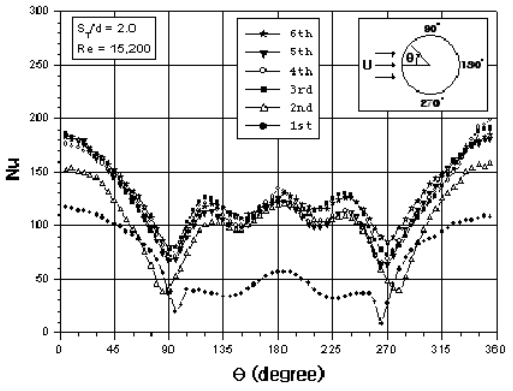

(a) $S_T/d = 2.0$

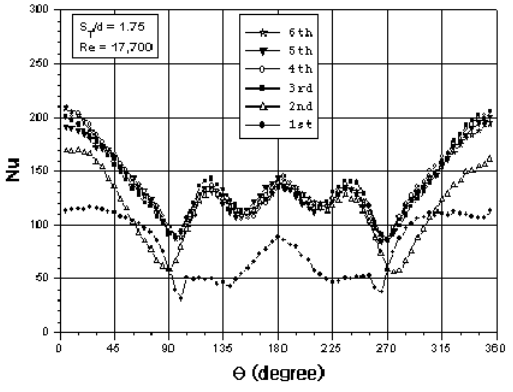

(b) $S_T/d = 1.75$

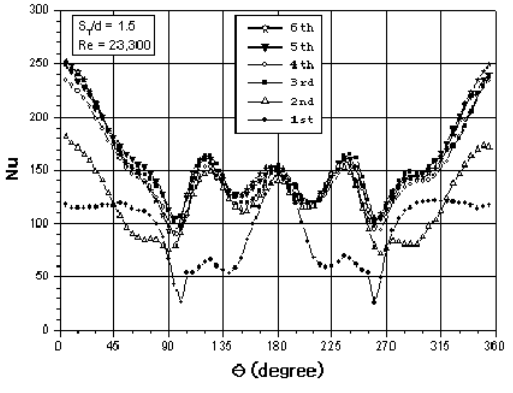

(c) $S_T/d = 1.5$

Fig. 3. Distribution of local Nusselt number at various tube locations for three cylinder spacings.

second and third tubes, respectively, in comparison with that of the first tube. In case of the first tube, the heat transfer coefficients near the front stagnation point are nearly equal for all tube spacings, but their distribution in the rear part is quite different. The local heat transfer coefficients near the rear stagnation point

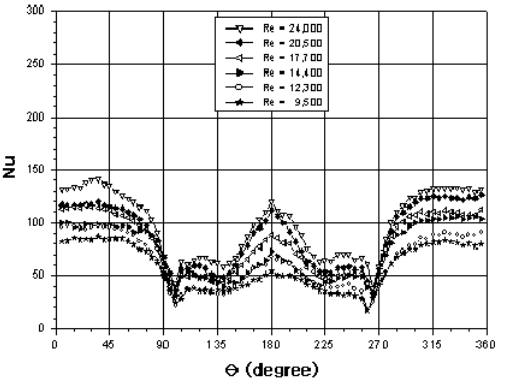

(a) first tube

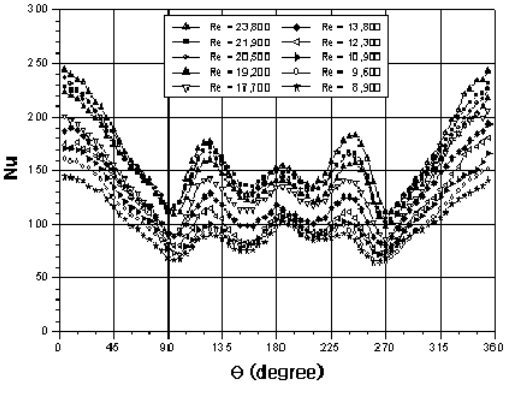

(b) third tube

Fig. 4. Variation of local Nusselt number with Reynolds number on the first and third tubes for $S_T/d = 1.75$.

increase drastically with decreasing tube spacing. As the tube spacing decreases, the size of recirculation zone formed in the rear part of the first tube becomes smaller, the intensity of the vortices becomes stronger, and thereby the heat transfer is augmented. Consequently, the average Nusselt number on the first tube for the tube spacing of 1.75 and 1.5 is higher by about 25% and 45% than that for the tube spacing of 2.0.

The local heat transfer on the first and third tubes is examined at various Reynolds numbers for three tube spacings, and one case for $S_T/d=S_L/d=1.75$ is presented in Fig. 4. As seen in the figure, for both the first and third tubes, the distribution pattern of the local heat transfer coefficients is similar regardless of the Reynolds number, and the local heat transfer coefficients increase gradually as the Reynolds number increases. In case of the third tube, the local Nusselt numbers near $\theta = 120°$ is lower than those of the rear stagnation point at relatively low Reynolds numbers, but this trend is reversed at high Reynolds number.

The variations of the local Nusselt numbers for both cases of $S_T/d=S_L/d=2.0$ and 1.5 are similar to that of $S_T/d=S_L/d=1.75$ although their results are not presented in this paper.

4.2 Average heat transfer characteristics

The average heat transfer coefficients on the first and third tubes are obtained by integrating the local heat transfer coefficient, and they are compared with the conventional heat transfer correlations.

Figure 5 shows the relation between the average Nusselt number and the Reynolds number on the first tube for three tube spacings. Dependence of Nusselt number on Reynolds number is almost same regardless of the tube spacing, and their empirical correlation can be expressed as in Eq. (8).

$$Nu = 0.271Re^{0.583} \tag{8}$$

This correlation is derived by the least square fitting of the experimental data, and the correlation coefficient is 0.991. The present correlation obtained using mass transfer experiments is compared with the heat transfer correlation of Aiba et al. (1982b) which is presented with the dotted line. In the Aiba's experiment, the tube spacing is 1.6, and the tube banks have 3 columns and 7 rows. Their experiments were conducted by heating only the test tube under the condition of constant heat flux. There is a little difference of slope between two correlations, but the error is less than 5% in the range of Reynolds numbers studied.

The average Nusselt numbers on the third tube at various Reynolds numbers are presented in Fig. 6. As in the case of the first tube, all the data are well fitted with one empirical correlation given in Eq. (9).

$$Nu = 0.511Re^{0.57} \tag{9}$$

The dotted lines are the correlations by Aiba et al. (1982b, $10^4 < \mathrm{Re} < 3.6\times10^4$) and Žukauskas (1972, $10^3 < \mathrm{Re} < 2\times10^5$, $0.7 < \mathrm{Pr} < 500$). Aiba's correlation was obtained from the average Nusselt numbers on the third tube, but Žukauskas' correlation is for tube banks with 16 or more rows. At relatively low Reynolds numbers, present data are somewhat higher than Aiba's correlation, but this trend is reversed with increasing Reynolds number. Although it is difficult to compare local values in detail with those of Aiba due to different experimental range of Reynolds number, relatively slow variations in the local heat transfer coefficient are found in Aiba's data. The difference of the local Nusselt numbers between heat

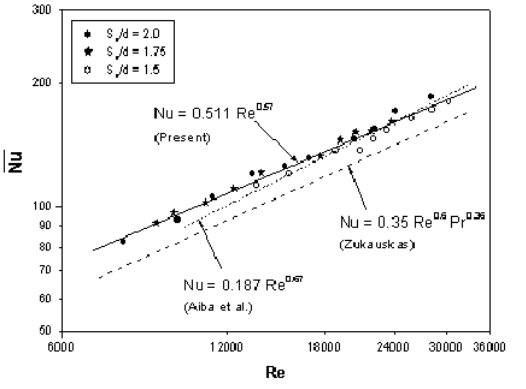

Fig. 6. Average Nusselt number versus Reynolds number on the third tube

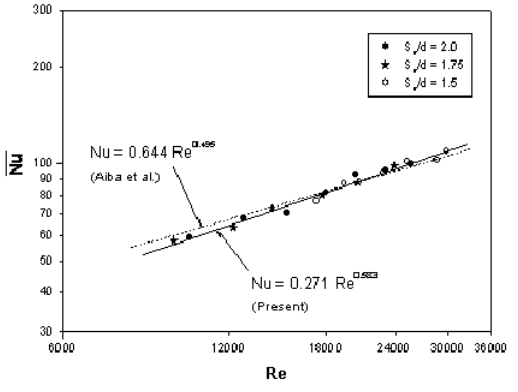

Fig. 5. Average Nusselt number versus Reynolds number on the first tube.

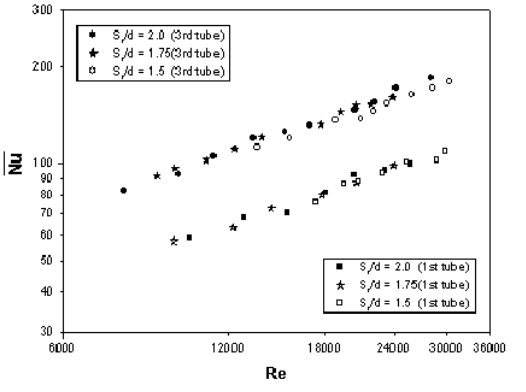

Fig. 7. Comparison of average Nusselt number versus Reynolds number between the first and third tubes.

and mass transfer experiments may be attributed to the conduction error and the effect of exponent n in the analogy equation. Nevertheless, present correlation is agreed with Aiba's within the maximum error of 8% in the Reynolds number studied. Meanwhile, present and Aiba's average heat transfer values are much higher than those obtained from Žukauskas' correlation. This is because Žukauskas' correlation was obtained by averaging Nusselt numbers for all tubes including the first and second tubes where heat transfer coefficients are much lower than the third tube.

In order to compare the average Nusselt numbers between the first and third tubes, the results of Figs. 5 and 6 are presented together in Fig. 7. In the range of Reynolds number examined, the average Nusselt numbers on the third tube are higher by about 65% than those of the first tube. As mentioned earlier, an obstacle does not exist in front of the first row, and thus the main flow approaches the first row without any disturbance. But in the second and subsequent rows, the oncoming velocity becomes almost double, and the flow is disturbed by the vortices of upstream tube. These cause an increase in the heat transfer on the third tube.

5. Conclusions

The heat transfer characteristics for staggered tube banks in cross-flow are investigated for various tube spacings, tube locations and Reynolds numbers using the naphthalene sublimation technique. Major results are summarized as follows:

1) For all tube spacings, the variation pattern of the local heat transfer coefficients is different from the first tube to the third tube, but they are similar afterwards where the flow is developed. And the average Nusselt number increases more than 30% and 65% on the second and third tubes, respectively, in comparison with that of the first tube.

2) The local heat transfer coefficients on each tube increase except on the front part of first tube as the tube spacing decreases.

3) The local heat transfer near the rear stagnation point of the first tube increases drastically with decreasing tube spacing due to strong vortices. Consequently, the average Nusselt number on the first tube for the tube spacing of 1.75 and 1.5 is higher by about 25% and 45%, respectively than that for the tube spacing of 2.0.

4) In the first and third tubes, dependence of average Nusselt number on Reynolds number is almost same regardless of the tube spacing. And the empirical correlations for average Nusselt number are well agreed with Aiba's correlations within the maximum error of 5% and 8% in the first and third tubes, respectively.

Acknowledgment

This study was supported in part by the Regional Research Center for Advanced Climate Control Technology at Sun-Moon University.

Nomenclature

A : Naphthalene sublimation area
D : Cylinder diameter
D_{iff} : Mass diffusion coefficient of naphthalene in air
h_m : Mass transfer coefficient
$\dot{m}$: Mass transfer rate
n : Exponent in Eq. (5)
Nu : Nusselt number
Pr : Prandtl number
Re : Reynolds number
Sc : Schmidt number
Sh : Sherwood number
S_L : Longitudinal distance between tube centers
S_T : Transverse distance between tube centers
U : Approaching velocity
U_{max} : Maximum velocity between tubes

Greek symbols

Δt : Sublimation depth
$\Delta \tau$: Total exposure time in the wind tunnel
θ : Circumferential angle from front stagnation point
ν : Kinematic viscosity of air
ρ_s : Density of solid naphthalene
$\rho_{v,w}$: Naphthalene vapor density on the surface
ρ_∞ : Naphthalene vapor density in the free-stream

References

Achenbach, E., 1989, "Heat Transfer from a Staggered Tube Bundle in Cross-Flow at High Reynolds Numbers," *Int. J. of Heat and Mass Transfer*, Vol. 32, pp. 271~280.

Aiba, S., Tsuchida, H., Ota, T., 1982a, "Heat Transfer

Around Tubes in In-line Tube Banks," *Bulletin of JSME*, Vol. 25, No. 204, pp. 919~926.

Aiba, S., Tsuchida, H., Ota, T., 1982b, "Heat Transfer Around Tubes in Staggered Tube Banks," *Bulletin of JSME*, Vol. 25, No. 204, pp. 927~933.

Ambrose, D., Lawrenson, I. J., Sprake, C. H. S., 1975, "The Vapor Pressure of Naphthalene," *J. of Chemical Thermodynamics*, Vol. 7, pp. 1173~1176.

Boulos, M. I., Pei, D. C. T., 1974, "Dynamics of Heat Transfer from Cylinders in a Turbulent Air Stream," *Int. J. of Heat and Mass Transfer*, Vol. 17, pp. 767~783.

Buyruk, E., 2002, "Numerical Study of Heat Transfer Characteristics on Tandem Cylinders, Inline and Staggered Tube Banks in Cross-Flow of Air," *Int. Communications in Heat and Mass Transfer*, Vol. 29, pp. 355~366.

Buyruk, E., Johnson, M. W., Owen, I., 1998, "Numerical and Experimental Study of Flow and Heat Transfer Around a Tube in Cross-flow at Low Reynolds number," *Int. J. of Heat and Fluid Flow*, Vol. 19, pp. 223~232.

Goldstein, R. J., Cho, H. H., 1995, "A Review of Mass Transfer Measurements Using Naphthalene Sublimation," *Experimental Thermal and Fluid Science*, Vol. 10, pp. 416~434.

Grimison, E. D., 1937, "Correlation and Utilization of New Data on Flow Resistance and Heat Transfer for Cross Flow of Gases Over Tube Banks," *Trans. of ASME*, Vol. 59, pp. 583~594.

Huge, E. C., 1937, "Experimental Investigation of Effects of Equipment Size on Convection Heat Transfer and Flow Resistance in Cross Flow of Gases Over Tube Banks," *Trans. of ASME*, Vol. 59, pp. 573~581.

Kim, M. S., Baek, B. J., Pak, B. C., 2000, "An Experimental Study of Fouling Effect on the Heat Transfer Around a Tube in Staggered Tube Banks," *Trans. of the KSME(B)*, Vol. 24, No. 11, pp. 1478~1485.

Kline, S. J., McClintock, F. A., 1953, "Describing Uncertainty in Single-Sample Experiments," *Mechanical Engineering*, Vol. 75, pp. 3~8.

Merker, G. P., Hanke, H., 1986, "Heat Transfer and Pressure Drop on the Shell-side of Tube-Banks Having Oval-shaped Tubes," *Int. J. of Heat and Mass Transfer*, Vol. 29, pp. 1903~1909.

Park, J., Kwon, K., Choi, H., 1998, "Numerical Solutions of Flow Past a Circular Cylinder at Reynolds Numbers up to 160," *KSME Int. J.*, Vol. 12, No. 6, pp. 1200~1205.

Pierson, O. L., 1937, "Experimental Investigation of the Influence of Tube Arrangement on Convection Heat Transfer and Flow Resistance in Cross Flow of Gases Over Tube Banks," *Trans. of ASME*, Vol. 59, pp. 563~572.

Scholten, J. W., Murray, D. B., 1998, "Heat Transfer and Velocity Fluctuations in a Staggered Tube Array," *Int. J. of Heat and Fluid Flow*, Vol. 19, pp. 233~244.

Son, J. S., Hanratty, T. J., 1969, "Velocity Gradients at the Wall for Flow Around a Cylinder at Reynolds Numbers from 5×103 to 105," *J. of Fluid Mechanics*, Vol. 35, pp. 353~368.

Žukauskas, A., 1972, Heat Transfer from Tubes in Crossflow, Advances in Heat Transfer, *Academic Press*, New York, Vol. 8, pp. 93~160.